Springer

Journal of
Mechanical
Science and
Technology

Journal of Mechanical Science and Technology 22 (2008) 621~627

www.springerlink.com/content/1738-494x

Mechanical behavior of arteries under inflation and extension

Taewon Kang*

School of Mechanical and Automotive Engineering, Kookmin University, Seoul, 136-702, Korea

(Manuscript Received August 31, 2006; Revised July 5, 2007; Accepted February 22, 2008)

Abstract

In order to understand the blood vessel of artery responding to medical treatments, there is a need to quantify the biomechanical behavior of the vessel. Using video dimension analyser, mechanical pressure-diameter relationships of passive carotid artery with and without balloon inflated at various axial loads were measured. Inversion test was also analytically modeled to address the heterogeneity of artery due to constituents. The pressure-diameter curves and stress distribution across the arterial wall were calculated. The simulation showed that the inversion tests, in comparison to other mechanical tests, provided additional information to develop the strain energy function describing arterial behavior

Keywords: Balloon angioplasty; Arterial wall; Inversion; Heterogeneity; Strain energy function

1. Introduction

The balloon angioplasty is widely used to increase the lumen of an obstructed vessel by the inflation of an intravascular balloon catheter. This technique encompasses a variety of procedures used to treat patients with diseased arteries of the heart, for example, chest pain caused by a build-up of fats, cholesterol, and other substances from the blood. Balloon angioplasty compacts the atheromatous material within a relatively unyielding artery comparing to a normal one, but the mechanisms of balloon angioplasty are very complicated and primarily related to mechanical behavior of arteries. Indeed, it appears that cells in the vessel tend to organize to achieve an optimal state of stress and strain [1]. This suggests that these mechanisms can be understood by employing mechanical tests and quantifying the changes in the mechanical behavior of arteries due to balloon angioplasty. However, not much of data on arterial behavior are available due to a few studies on vessel mechanics and most data have come from the histological studies [2, 3].

The histology reveals that the primary mechanisms are overstretching of media and splitting of the plaque and intima. Since the plaques are associated principally with intima, the media and the adventitia exhibit nearly normal biomechanical behavior of vessels [4]. Thus studies on normal arteries will provide useful information to the understanding of balloon-induced overstretching of the vascular wall. The first aim of this study is to identify the differences of normal passive vessels before and after balloon angioplasty.

Elastic arteries are consisted of three layers. It is widely accepted that the media with primarily smooth muscles and the adventitia with mainly collagen fibers are the primary load bearing layers. Since the heterogeneity of the arterial wall has not been investigated intensively, there is a need to address their properties separately [5, 6]. Quantification of the mechanical properties of arteries may be best accomplished using a pseudo-elastic approach [7]. Also, the availability of general solutions to the boundary value problems is fundamental to the identification of constitutive relations. By inversion, the spatial location of the media and the adventitia is reversed and this may provide additional information on the heterogeneous

*Corresponding author. Tel.: +82 2 910 5451, Fax.: +82 2 910 4839
E-mail address: jirehk@kookmin.ac.kr
DOI 10.1007/s12206-008-0213-3

properties of the arterial wall. Thus, the second aim of this study is to present the finite extension and inflation of an inverted artery as a useful information for developing a form of strain energy function.

2. Materials and methods

2.1 Experimetal methods

Before attempting vessels in the heart, common carotid arteries were selected as specimens due to their geometrical simplicity. The arteries were obtained from 11 canines with age and weight variations and kept in a physiological salt solution (PSS). Experiments were carried out within 1-2 days while the mechanical properties remain unchanged [8]. Each vessel was cut into 3-4 cm long and the selected segments had nearly uniformed diameter. A 1 mm thick ring of the artery was cut from one end of the specimen for measuring inner and outer diameters in the unloaded state. The remainder of the vessel was cannulated at both ends.

The cannulated vessel was suspended vertically from a ring stand. One cannula was connected to a pressure transducer and a syringe whereas precision weights were hung from the other cannula so that the vessel was maintained the constant length during perfusion. Deformations in a central gage length of the cannulated vessel were monitored by a computer-based video system including video dimension analyser. Also, data for the outer diameter of vessel was collected during inflations.

The cannulated vessel was cyclically inflated/ deflated with the PSS from 0-200 mmHg at ≃ 0.1 Hz and at various levels of constant axial load (5 and 25 grams). Following preconditioning, the pressure, diameter and gage length were measured on-line at 30 Hz and transferred on disc for off-line analysis. Once these "control" protocols were finished, a 5 mm outer-diameter balloon catheter was inserted into the vessel and inflated the specimen three times to 3 atm for 90 seconds as performed in clinical surgery. Then, the catheter was withdrawn and the cyclic protocols of inflating and deflating were repeated for each of the constant axial loads. All protocols were performed at room temperature, and the outer surface of specimen was kept moist with the PSS.

2.2 Analytical modeling

In addition to inflation and deflation test protocols performed on arteries, it is desired to add more insight into arterial behavior due to heterogeneity based on theoretical simulations.

The theoretical modeling starts with the consideration of residual stress. Residual stress is the stress that remains in a body after removal of external loads. When one introduces a radial cut in an arterial segment, the segment opens up. Fung suggested that this was the evidence of residual stress existing in arteries [9]. It is believed that the residual stress is due to growth and remodeling of vessel. One of the important role of residual stress is to reduce the transmural distribution of stresses across the arterial wall [10].

The next step is to build the successive finite deformation of an artery from a cut, stress-free reference state, to an unloaded intact state, to an unloaded inverted state, and finally to finitely deformed state of inverted artery as shown in Fig. 1.

The motion associated with the deformation gradient F_1 is,

$$\rho = \rho(R), \theta = (\frac{\pi}{\Theta_O}) \times \Theta, \varsigma = \lambda Z \qquad `(1)$$

where Θ_O is the opening angle and λ is the axial stretch ratio associated with the residual stress. The motion associated with F_2 is,

$$\rho^* = \rho^*(\rho), \theta^* = \pi - \theta, \zeta^* = \delta\zeta \qquad (2)$$

where δ is a possible axial stretch ratio due to the inversion alone. The motion associated with F_3 is,

$$r = r(\rho^*), \Theta = \theta^*, z = \Lambda\zeta^* \qquad (3)$$

where Λ is an axial stretch ratio in loaded state.

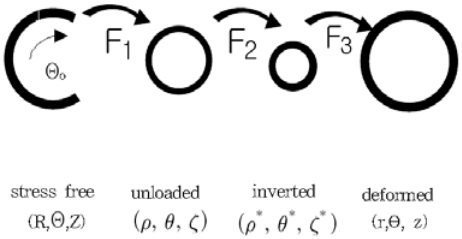

Fig. 1. Schematic of arterial cross-sections in various configurations.

The final deformation gradient tensor is **F**= $F_3 \bullet F_2 \bullet F_1$, and the associated physical components of **F** are, in matrix form,

$$F_{iA} = \begin{vmatrix} \dfrac{dr}{dR} & 0 & 0 \\ 0 & -\dfrac{r\pi}{R\Theta_O} & 0 \\ 0 & 0 & \delta\lambda\Lambda \end{vmatrix} \tag{4}$$

The incompressibility constraint requires that determinant of **F** has to be 1, which leads to the equation,

$$r_i^2 - r_a^2 = \frac{\Theta_O}{\pi\lambda\delta\Lambda}(R_a^2 - R_i^2) \tag{5}$$

where R_i and R_a denote the intimal and adventitial radii in the stress-free state. Similarly, r_i and r_a denote the intimal and adventitial radii in externally deformed state. Since $R_a > R_i$ Eq. (5) reveals that $r_i > r_a$. Therefore, the location of adventitia and intima is reversed and the final deformation describes the inversion correctly.

Components of the Cauchy stress t are easily found provided that the pseudo-strain energy function W is known. A general constitutive relation for an incompressible,nonlinearly pseudoelastic, anisotropic material undergoing finite deformation is [11],

$$t = -PI + 2F \cdot \frac{\partial W}{\partial C} \cdot F^T \tag{6}$$

where $C(= F^T \cdot F)$ is the right Cauchy-Green deformation tensor, P is a Lagrange multiplier and I is the identity tensor.

For the inflation and extension of an inverted artery, the requisite equilibrium equations are, assuming a closed-end artery,

$$P_i = \int_{r_a}^{r_i} (t_{\theta\theta} - t_{rr}) \frac{dr}{r} + P_{o,} \tag{7}$$

$$L = \int_{r_a}^{r_i} (2t_{zz} - t_{rr} - t_{\theta\theta}) r dr - P_i \pi r_a^2 \tag{8}$$

where P_i and P_o are luminal and outer pressures and L is the applied axial load in the final state. These equations can be used to calculate the stress distribution in the wall of the inverted artery.

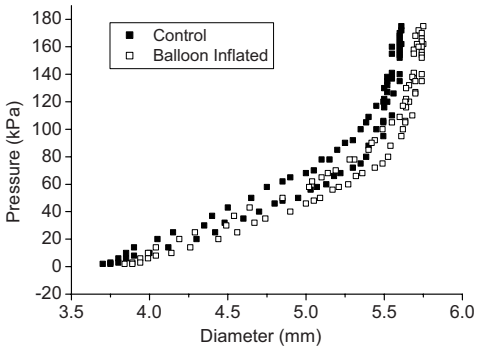

Fig. 2. Comparison of control and balloon induced vessel behavior (axial weight is 25 gram).

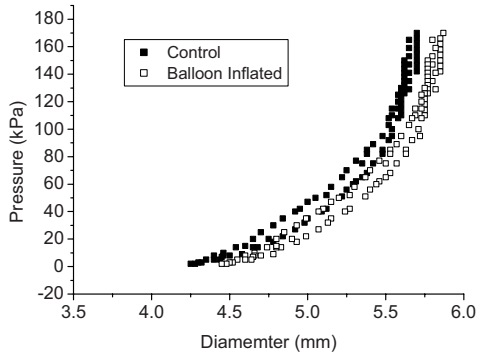

Fig. 3. Comparison of control and balloon induced vessel behavior (axial weight is 5 gram).

3. Results and discussion

3.1 Experimental data

As seen in other soft tissues [12], all 11 vessels exhibited similar behavior, including hysteresis and a nonlinear pseudoelastic response. Fig. 2 shows the pressure-diameter behavior for one specimen both before and after balloon dilation at constant axial load of 25 gram.

The arterial behavior due to inflation was almost the same at low pressure, but when pressure was increased to higher values the balloon induced specimen was dilated wider.

Fig. 3 also shows the pressure-diameter behavior for one specimen both before and after balloon dilation at constant axial load of 5 gram.

The characteristics of balloon dilated vessel in Fig.

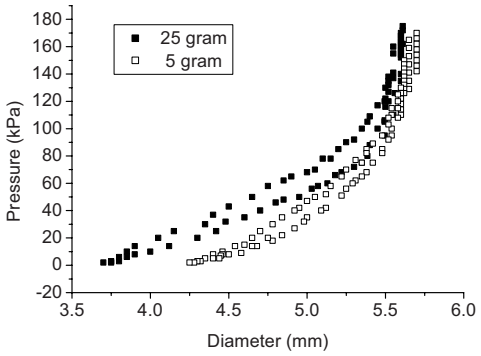

(a) Control vessel

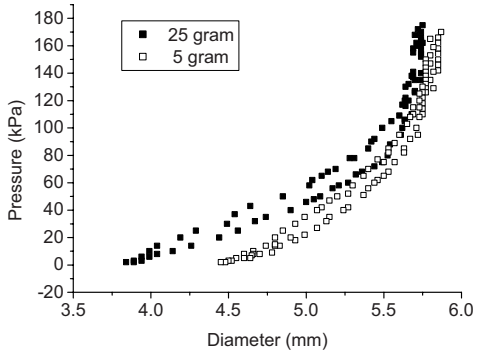

(b) Balloon-induced vessel

Fig. 4. Comparison of vessel behavior (axial weights are 5 gram and 25 gram, respectively).

3 was very similar to the one in Fig. 2. Due to the increased axial load, the initial outer diameter was smaller, but the outer diameter at higher pressure became close to one at different axial loads.

These data show that there is a consistent shift in the outer diameter of the balloon inflated vessels. This means an acute weakening, or damage, of the vessel wall.

Also, as shown in Fig. 4(a) and (b), both the control and the balloon-induced vessels showed that they stiffened with the increased axial loads. Both initial outer diameters with higher axial weights are smaller and the required pressures to maintain the larger diameters are higher with increased axial weights.

3.2 Comparison to other mechanical studies

Consigny et al performed uniaxial extension tests on rings taken from rabbit iliacs; right one for normal test and left one for balloon inflated test [2]. Data were collected for both the passive and active state. However, it was not a true set of pressure-diameter data since force-extension data on ring tests must be converted into "equivalent" pressure-diameter data. Moreover, Cox showed that data from ring segments imply a "significant stiffer" behavior than data from intact cylindrical segments [13]. This supports the protocols on cylindrical vessel since the in-vivo geometry, ultrastructure and loading conditions are preferable.

It is believed that pressure-diameter data are useful to qualitatively evaluate the behavior of normal and balloon inflated vessels separately at various levels of axial load.

3.3 Computer Simulations

If a material is elastic and has a strain energy function W, engineers can calculate the stress from W. The form of strain energy function for biological material is not simple due to the complicated internal energy and the free energy. Schulze-Bauer and Holzafel proposed a constitutive equation from the pressure diameter relations and a strain energy function for membrane modeling [14]. Gundiah et al used the Mooney-Rivlin strain energy function to describe the material properties of elastin [15]. However, those models are not sufficient to explain the vessel heterogeneity. Fung introduced a potentially useful strain energy function for the complicated material symmetry [16].

In order to show that "inversion" tests provide additional information on the heterogeneity of the arterial wall, a strain energy function which was introduced by Fung is used to calculate the stress. For the purpose of illustration, consider the finite deformation of a normal and an inverted artery, described by a strain energy function of the form $W = c[e^{Q} - 1]$ with,

$$Q = b_1 E_{\Theta\Theta}^2 + b_2 E_{ZZ}^2 + b_3 E_{RR}^2 + 2b_4 E_{\Theta\Theta} E_{ZZ} \tag{9}$$

wherein the material constants in the paper of Chung and Fung [17] were employed since there is no general form of constitutive equations for control and balloon-damaged arteries : c= 22.4kPa, b_1=1.0672, b_2=0.4775, b_3=0.0499, b_4=0.0903, b_5=0.0585 and b_6=0.0042. In addition, we let R_i=3.92 mm, R_a=4.5 mm, T_o=71.4°, λ=1.017695, and d=1.07.

Shown in Fig. 5(a) are simulated pressure versus deformed inner radius (for normal and for inverted) data for an inflation test at a constant Λ. Fig. 5(b) shows the axial load versus stretch data for an extension test at a constant diameter. It shows also the dif-

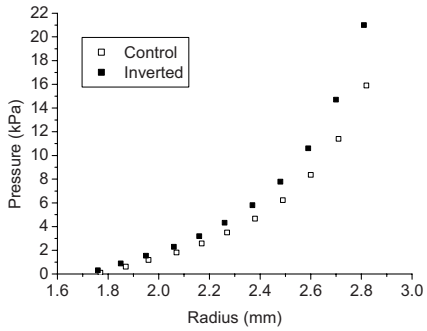

(a) Constant stretch ratio test

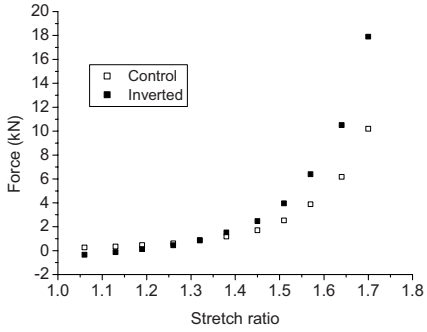

(b) Constant diameter test

Fig. 5. Comparison of simulated control and inverted arteries.

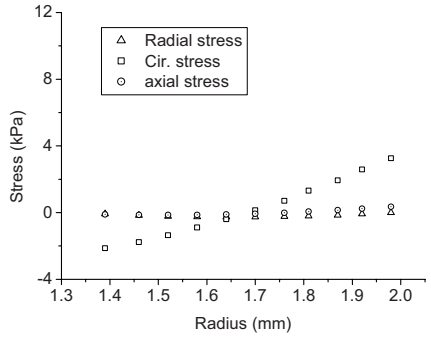

(a) Stress distribution of normal vessel

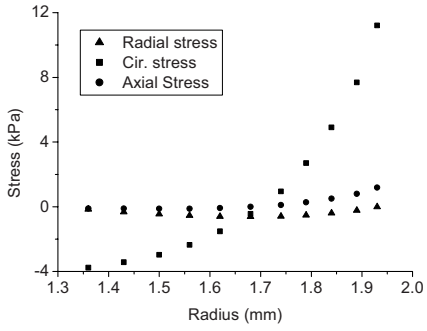

(b) Stress distribution of inverted vessel

Fig. 6. Transmural stress distribution of normal and inverted vessel at unloaded states.

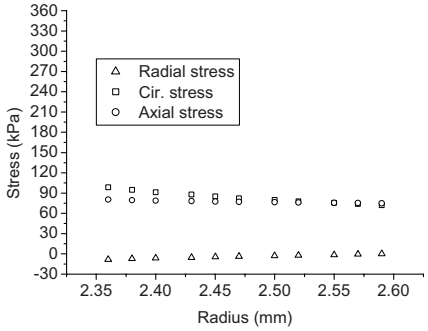

(a) Stress distribution of normal vessel

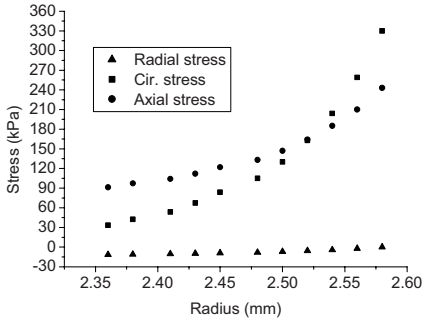

(b) Stress distribution of inverted vessel

Fig. 7. Transmural stress distribution of normal and inverted vessel at loaded states.

ference between control and inverted states.

Values of the Cauchy stress **t** in unloaded normal and inverted states are shown in Fig. 6(a) and 6(b), respectively.

Shown in Fig. 7(a) and (b) are the simulated stress distribution across the wall in a loaded (inner pressure = 80 mmHg, and a stretch ratio = 1.69) normal and inverted state.

3.4 Simulation analysis

Fig. 5 suggests that the general characteristics of the global behavior of control and inverted artery based on Eq. (9) are similar to the arterial behavior described in Figs. 2 and 3. However, an inversion test could yield additional information to understand the vessel behavior since the inverted vessel appears to be slightly stiffer whereas the artery weakens after the balloon dilation. The similar understanding can be inferred from Figs. 6 and 7.

The stress distribution in Fig. 6(a) and (b) for unloaded normal and inverted states are similar except for the circumferential stress. However, the stresses in the loaded normal and inverted states are

significantly different. Both the circumferential and axial stresses are increased monotonically from the inner to the outer wall in the inverted artery (Fig. 7(b)). This is a sharp contrast to the familiar stresses in normal artery decreasing across the wall (Fig. 7(a)).

Since the intimal stretch ratio becomes large due to the inversion, that the circumferential stress is much larger in the outer wall (which is intima) of the inverted vessel is not surprising. Moreover, it is reasonable that $t_{\Theta\Theta}$ is less in the inner wall of an inverted vessel since the inversion results in a lower value of the adventitial λ_Θ; this λ_Θ can remain < 1 even at low pressures.

As seen in Figs. 5, 6 and 7 for a homogeneous vessel described by the Chuong/Fung strain energy function, an inversion test can yield data that are different, but complementary to the normal extension and inflation tests. Since arterial wall is layered, and since the inversion reverses the spatial location of these layers, it is possible that these tests will be particularly useful in quantifying the heterogeneity of the wall. That is, when combined with the normal inflation and extension tests, inversion data may allow more robust estimates of the best-fit material parameters separately for the media and adventitia. Therefore, an inversion test is necessary to get better understanding of mechanisms on heterogeneous vascular wall which responds to the structural and functional changes induced by the clinical treatments.

4. Conclusions

Pressure-diameter data were used to qualitatively evaluate the behavior of normal and balloon inflated vessels separately at various levels of axial loads. The data revealed that the vessel after balloon angioplasty became weaker due to damage. These and additional data are very important for identifying the general characteristics of the mechanical mechanism of balloon angioplasty.

Inversion tests are shown to be useful in describing the vessel behavior qualitatively and quantitatively. Before attempting to collect more experimental data from inversion tests, it requires to identify the general characteristics of arterial behavior. Thus, once the general characteristics are known, it is believed that inversion tests as well as other novel testing procedures will be appropriate and useful for developing a strain energy function to describe the heterogeneity of vessel. Moreover, these tests will contribute to the development of nonlinear finite element models so that the complicated geometries and boundary conditions can be well addressed.

Reference

[1] S. C. Cowin, How is tissue built? *J. of Biomechanical Engr*., 122 (2000) 553-569.

[2] P. M. Consigney, T. N. Tulenko and R. F. Nicosia, Immediate and long term effects of angioplasty-balloon dilation on normal rabbit iliac artery, *Arteriosclerosis*, 6 (3) (1986) 265-276.

[3] P. M. Consigny and R. F. LeVeen, Effect of angioplasty balloon inflation time on arterial contractions and mechanics, *Investigative Radiology*, 23 (1988) 271-276.

[4] G. L. Wolf, R. F. LeVeen and E. J. Ring, Potential mechanisms of angioplasty, *Cardiovascular and Interventional Radiology*, 7 (1984) 11-17.

[5] W. W. von Maltzahn, R. G. Warriyar and W. F. Keitzer, Experimental measurements of elastic properties of media and adventitia of bovine carotid arteries, *J Biomech*, 17 (1984) 839-847.

[6] H. Demiray and R. P. Vito, A layered cylindrical shell model for an aorta, *Int J Engr Sci*, 29 (1990) 47-54.

[7] J. D. Humphrey, R. K. Strumpf and F. C. P. Yin, A theoretically-based experimental approach for identifying vascular constitutive relations, *Biorheol*, 26 (1989) 687-702.

[8] P. B. Dobrin and T. R. Canfield, Elastase, collagenase, and the biaxial elastic properties of dog carotid artery, *American Journal of Physiology*, 247 (1984) H124-H131.

[9] C. J. Chuong and Y. C. Fung, On residual stress in arteries, *J Biomech Engr*, 108 (1986) 189-192.

[10] J. D. Humphrey and S. L. Delange, An Introduction to Biomechanics: Solids and Fluids, Analysis and Design. Springer, New York, (2004).

[11] J. D. Humphrey, Cardiovascular solid mehanics: cells, tissues, and organs. Springer, New York, (2002).

[12] Y. C. Fung, Biomechanics: Mechanical Properties of Living Tissues. Second Edition. Springer-Verlag, New York, (1993).

[13] R. H. Cox, Comparison of arterial wall mechanics using ring and cylindrical segments, *Am J Physiol*, 244 (1983) H298-H303.

[14] C. A. J. Schulze-Bauer and G. A. Holzafel, Determination of constitutive equations for human arter-

ies from clinical data, *J of Biomechanics*, 36 (2003) 165-169.

[15] N. Gundiah, M. Ratcliffe and L. A. Pruitt, accepted, Determination of strain energy function for arterial elastin: experiments using histology and mechanical tests, *J. of Biomechanics.*

[16] Y. C. Fung, Biomechanics: Motion, Flow, Stress, and Growth. Second Edition. Springer-Verlag, New York, (1990).

[17] C. J. Chuong and Y. C. Fung, Three dimensional stress distribution in arteries, *J Biomech Engr*, 105, (1983) 268-274.